potential of the $Cu|Cu^{2+}$ redox system, thus preventing the large-scale deposition of Cu as well as the dissolution of the deposited Cu dots. An elliptical Pt wire about 50 μm in diameter was used as a tool, which is reflected in the elliptical shape of the dots. For the formation of Cu crystallites on the Au surface, a nucleation barrier has to be surmounted (*22*), requiring a critical Cu adatom concentration on the Au surface during the pulse. This kinetic constraint assists the strongly localized Cu deposition.

The versatility of electrochemical reactions, combined with spatial resolution down to the nanometer range, may provide new abilities for modern micromachining technologies. Electrochemical microstructuring is not restricted to sequential fabrication. Complicated structures could be molded directly onto a surface using an appropriately shaped tool. The theoretically achievable spatial resolution compares favorably with that of state-of-the-art lithographical techniques, with the additional advantage of fully 3D capabilities.

**References and Notes**


1. P. Rai-Coudhury, Ed., *Handbook of Microlithography, Micromachining, & Microfabrication* (SPIE Optical Engineering Press, Bellingham, WA, 1997).
2. I. Amato, *Science* **282**, 402 (1998).
3. M. A. Burns *et al.*, *Science* **282**, 484 (1998).
4. J. T. Santini, M. J. Cima, R. Langer, *Nature* **397**, 335 (1999).
5. H. Jerman and S. Terry, in (*1*), vol. 2, pp. 379–434.
6. M. U. Kopp, A. J. d. Mello, A. Manz, *Science* **280**, 1046 (1998).
7. K. Jensen, *Nature* **393**, 735 (1998).
8. C. R. Friedrich *et al.*, in (*1*), vol. 2, pp. 299–378.
9. R. M. Nyffenegger and R. M. Penner, *Chem. Rev.* **97**, 1195 (1997).
10. A. J. Bard, G. Denuault, C. Lee, D. Mandler, D. O. Wipf, *Acc. Chem. Res.* **23**, 357 (1990).
11. W. Li, J. A. Virtanen, R. M. Penner, *Appl. Phys. Lett.* **60**, 1181 (1992).
12. W. Li *et al.*, *J. Phys. Chem.* **100**, 20103 (1996).
13. R. T. Pötzschke, C. A. Gervasi, S. Vinzelberg, G. Staikov, W. J. Lorenz, *Electrochim. Acta* **40**, 1469 (1995).
14. R. Schuster, V. Kirchner, X. H. Xia, A. M. Bittner, G. Ertl, *Phys. Rev. Lett.* **80**, 5599 (1998).
15. D. Hoffmann, W. Schindler, J. Kirschner, *Phys. Rev. Lett.* **73**, 3279 (1998).
16. D. M. Kolb, R. Ullmann, T. Will, *Science* **275**, 1097 (1997).
17. C. Lebreton and Z. Z. Wang, *J. Vac. Sci. Technol. B* **14**, 1356 (1996).
18. P. Avouris, T. Hertel, R. Martel, *Appl. Phys. Lett.* **71**, 285 (1997).
19. G. Milazzo, *Electrochemistry* (Elsevier, Amsterdam, 1963).
20. J. O. M. Bockris and A. K. N. Reddy, *Modern Electrochemistry* (Plenum, New York, 1970), vol. II.
21. H. Gerischer, *Electrochim. Acta* **35**, 1677 (1990).
22. M. A. Schneeweiss and D. M. Kolb, *Phys. Stat. Sol. (a)* **153**, 51 (1999).



23. We thank K. Grabitz, G. Heyne, J. Lehnert, and V. Platschkowski for technical support and D. Kolb for discussions.

5 April 2000; accepted 19 May 2000


# Taming Superacids: Stabilization of the Fullerene Cations $HC_{60}^+$ and $C_{60}^{\cdot+}$


**Christopher A. Reed,* Kee-Chan Kim, Robert D. Bolskar, Leonard J. Mueller**



**A new superacid, $H(CB_{11}H_6X_6)$ (where X = chlorine or bromine), whose conjugate base is the exceptionally inert $CB_{11}H_6X_6^-$ carborane anion, separates Brønsted acidity from oxidizing capacity and anion nucleophilicity in a manner not previously achieved. Reaction of this superacid with $C_{60}$ gives $HC_{60}^+$ as a stable ion in solution and in the solid state. In a separate experiment, an oxidant was developed such that the long-sought $C_{60}^{\cdot+}$ ion can be synthesized in solution. The preparation of these two fullerene carbocations is a notable departure from the prevalent chemistry of $C_{60}$, which is dominated by the formation of anions or the addition of nucleophiles. The $H(CB_{11}H_6X_6)$ superacid overcomes the major limitations of presently known superacids and has potentially wide application.**


Superacids (those stronger than 100% sulfuric acid) have been of great value to chemistry. In organic chemistry, superacidity has been used to stabilize carbocations such as $R_3C^+$ and $HCO^+$ and to study acid-catalyzed processes (*1, 2*). In inorganic chemistry, the oxidizing capacity of superacids has been widely exploited to stabilize unusual reactive cations such as $S_8^{2+}$, $Ir(CO)_6^{3+}$, and $Xe_2^+$ (*3–6*). Nevertheless, currently known superacids have limitations. For example, the anions of superacids ($SbF_6^-$, $HSO_4^-$, $CF_3SO_3^-$, and so forth) are too nucleophilic to allow the free silylium ion ($R_3Si^+$) to exist (*7*), and attempts to protonate and/or oxidize $C_{60}$ with superacids have led to its decomposition (*8*). Indeed, it is the combination of anion nucleophilicity and oxidizing capacity together with acidity that makes superacids corrosive and destructive, and limits many academic and industrial applications. Even the ostensibly nonoxidizing superacid triflic acid ($CF_3SO_3H$) decomposes $C_{60}$ (*9*).

If a superacid could be developed which was oxidant-free and whose conjugate base was significantly less nucleophilic than presently available anions, many desirable protonation reactions might be carried out without decomposition. Here, we report the preparation of a superacid, $H(CB_{11}H_6X_6)$ (X = Cl, Br), that meets these requirements and illustrate its use in stabilizing the previously unobserved $HC_{60}^+$ ion. We also show that the oxidizing capacity of superacids can be separately harnessed to the conjugate base ($CB_{11}H_6X_6^-$) to prepare an oxidant capable of producing the $C_{60}^{\cdot+}$ cation. $C_{60}$ has been referred to as the "electrophile par excellence" (*10*) because its dominant chemistry is the addition of nucleophiles or electrons (for example, $C_{60}^{n-}$ for $n$ = 1 to 6). Thus, the addition of an electrophile or the removal of an electron to form $HC_{60}^+$ and $C_{60}^{\cdot+}$, respectively, presents a particular challenge for synthetic chemistry and an excellent test for the concept of strict separation of oxidation from acidity and nucleophilicity.

Superacidity can be generated from a nonsuperacidic Brønsted acid by addition of a strong Lewis acid. A typical example is the addition of $SbF_5$ to HF to generate the common superacid $HSbF_6$, properly formulated as $[H(HF)_x^+][nSbF_5 \cdot SbF_6^-]$ (*4*). Here, we exploit the potent Lewis acidity of the silylium ion ($R_3Si^+$) to generate superacidity from HCl. Latent silylium ions are found in the silylium ion–like species $R_3Si(CB_{11}H_6X_6)$ (*7*) where $CB_{11}H_6X_6^-$ is the exceptionally inert and weakly nucleophilic anion shown in Fig. 1 (*11*). Condensing liquid HCl onto solid $(C_2H_5)_3Si(CB_{11}H_6X_6)$ at low temperature followed by removal of the volatiles under vacuum at room temperature yields the desired acid $H(CB_{11}H_6X_6)$ in essentially quantitative yield (Eq. 1).

$$(C_2H_5)_3Si(CB_{11}H_6X_6)_{(s)} + HCl_{(\ell)} \rightarrow H(CB_{11}H_6X_6)_{(s)} + (C_2H_5)_3SiCl_{(g)} \quad (1)$$

The absence of a AgCl precipitate when the product is dissolved in aqueous $AgNO_3$ shows that the possible alternative formulation of a HCl-solvated proton in $[H(HCl)_x^+][CB_{11}H_6X_6^-]$ can be discounted. For X = Br, the acid can be successfully sublimed under vacuum ($10^{-7}$ kPa) at 185°C to give a reasonable yield (45%) of white crystalline solid


Department of Chemistry, University of California, Riverside, CA 92521–0403, USA.

*To whom correspondence should be addressed. E-mail: chris.reed@ucr.edu

of high analytical purity [calculated (experimental) percentages for $CH_7B_{11}Br_6$: C, 1.75 (1.94); H, 1.23 (1.14); B, 18.95 (19.26); Br 76.90 (77.65)]. For an anion with hydridic B–H bonds, the carborane shows remarkable resilience toward acid and thermal decomposition. Infrared (IR) spectra (KBr or Nujol mull) show only bands due to the carborane anion (Fig. 2A, for X = Cl), and their frequencies are all within 2 to 3 $cm^{-1}$ of those in ionic carboranes. This result indicates that the symmetry of the anion is not greatly perturbed by protonation. The proton is probably located on a triangular face of halide substituents. Analysis by $^1H$ magic-angle-spinning (MAS) nuclear magnetic resonance (NMR) spectroscopy reveals an appropriately downfield-shifted resonance at 15.1 ppm that is assigned to the acidic proton. When treated with benzene vapor, the acid is cleanly converted to the known, remarkably stable (*12*), benzenium ion salt $[C_6H_7^+][CB_{11}H_6Cl_6^-]$ (Fig. 2B). It takes several orders of magnitude of acidity above $H_2SO_4$ to protonate benzene (*13*), so $H(CB_{11}H_6X_6)$ readily qualifies as a superacid and is appreciably stronger than triflic acid.

Treatment of a magenta solution of $C_{60}$ with one equivalent of $H(CB_{11}H_6Cl_6)$ in dry *o*-dichlorobenzene (ODCB) gives a claret red solution. The electronic absorption spectrum (Fig. 3B) shows a threefold increase in intensity in the visible region, consistent with broken icosahedral symmetry and greater allowedness of the forbidden electronic transitions of $C_{60}$. More diagnostically, near-IR bands at 754 and 1027 nm are closely similar to those of the recently reported carbocation $RC_{60}^+$ (R = $CHCl_2$) (*14, 15*).

The protonation of $C_{60}$ is reversible. Exposure of the solution to a base via aerobic moisture or by the addition of $Na_2CO_{3(s)}$ returns the spectrum to that of $C_{60}$. The room-temperature 500-MHz NMR characterization of $HC_{60}^+$ indicates fluxional behavior, with the proton "globe-trotting" rapidly over the $C_{60}$ sphere, presumably via 1,2 shifts. Thus, the $^{13}C$ signal of $C_{60}$ at 142.85 ppm in ODCB remains a singlet upon addition of $H(CB_{11}H_6Cl_6)$ and moves a mere 0.08 ± 0.01 ppm downfield (Fig. 4). This chemical shift is consistent with time-averaging of the spread of signals expected for a static structure, as observed with $RC_{60}^+$ (*14*). Fluctionality persists down to –70°C. A singlet at 6.6 ppm in the $^1H$ NMR spectrum is assigned to the C–H resonance of $HC_{60}^+$. This $sp^3$-C-H proton is highly deshielded but is not unlike those of the fullerene hydrocarbon $H_2C_{60}$ (5.9 ppm in toluene) (*16*). It is ~1 ppm downfield of comparable acidic protons in protonated benzene (5.6 ppm) (*17*). The resonance disappears upon addition of base and is absent in ODCB solutions of $H(CB_{11}H_6Cl_6)$. (The superacid also collapses the resonances of the solvent at 7.2 and 7.4 ppm into a broad asymmetric peak at 7.4 ppm, indicating facile protonation of ODCB.)

Analytically pure samples of solid $[HC_{60}][CB_{11}H_6Cl_6]$ can be produced by evaporating the solvent under vacuum. The four IR-active bands of $C_{60}$ (527 *vs*, 576 *s*, 1182 *s*, 1428 *s*) change their relative intensities in a manner typical of derivatization (*vs*, *m*, *m*, and *m*, respectively; see asterisk in Fig. 2C) but the frequencies are unchanged within spectral resolution (1 to 2 $cm^{-1}$). New weak bands appear at 545, 550, 560, and 612 $cm^{-1}$ that are also typical of $C_{60}$ derivatization. For example, in the [2+2] dimer $(C_{60})_2$ (*18*), weak bands are observed at 545, 551, 560, and 612 $cm^{-1}$. The proton-decoupled $^{13}C$ MAS NMR spectrum of $[HC_{60}][CB_{11}H_6Cl_6]$ (Fig. 5E) shows that the cation has a static structure in the solid state. A singlet at 56 ppm is assigned to the unique $sp^3$ C atom at the protonated site, a singlet at 182 ppm to the carbocation center, and a cluster of resonances in the 133 to 154 ppm range to the remaining 28 different sites expected from a $C_s$ symmetry structure. The proton attached to the 56 ppm C site must be isolated from other H atoms in the lattice because it can be observed at 6.6 ppm in the $^1H$ MAS NMR spectrum. Two-dimensional $^1H$-$^{13}C$ correlation experiments identify the 56 ppm $^{13}C$ resonance with this $^1H$ resonance. Using $^1H$-$^{13}C$ cross-polarization experiments with short contact times, the C nuclei closest to this proton can be identified (Fig. 5, A and B). With longer contact times (Fig. 5, C and D), enhancement of the peak at 182 ppm occurs, indicating a 1,4 (rather than 1,2) disposition of the cationic center. A classical carbocation of $C_s$ symmetry is suggested by these data (Scheme 1).

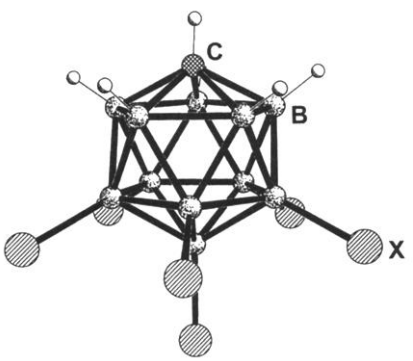


**Fig. 1.** Structure of the hexahalocarborane anion, $CB_{11}H_6X_6^-$ (X = Cl, Br).

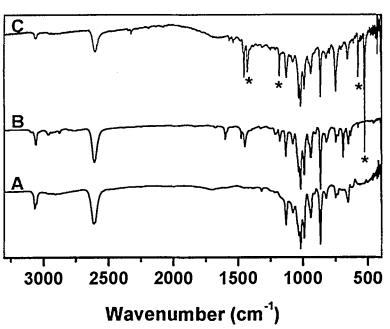


**Fig. 2.** Infrared spectra (KBr disk) of (**A**) $H(CB_{11}H_6Cl_6)$, (**B**) $[C_6H_7^+][CB_{11}H_6Cl_6^-]$, and (**C**) $[HC_{60}^+][CB_{11}H_6Cl_6^-]$. For meaning of asterisks, see text.

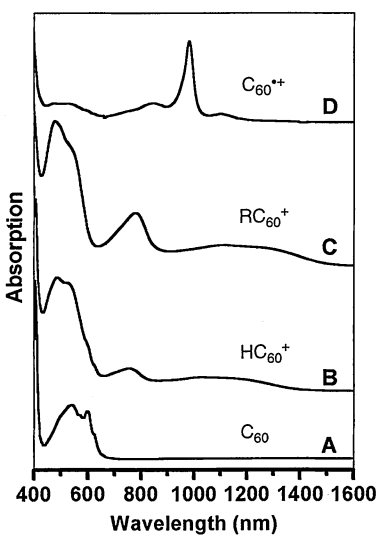


**Fig. 3.** Electronic spectra of (**A**) $C_{60}$ in ODCB, (**B**) $HC_{60}^+$ in ODCB, (**C**) $(CHCl_2)C_{60}^+$ in $CH_2Cl_2$, and (**D**) $C_{60}^{\cdot+}$ in TCE solution.

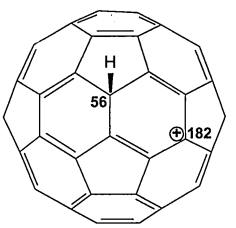


**Scheme 1.**

$C_{60}$ is very difficult to oxidize to $C_{60}^{\cdot+}$ in condensed media [the $C_{60}^{0/+}$ redox potential is +1.26 V versus ferrocene/ferrocenium in 1,1,2,2-tetrachloroethane (TCE) solution (*19*) (~1.7 V versus saturated calomel electrode or standard H electrode)].

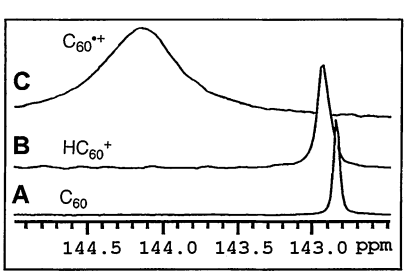


**Fig. 4.** Solution $^{13}C$ NMR spectra of (**A**) $C_{60}$ in ODCB, (**B**) $HC_{60}^+$ in ODCB, and (**C**) $C_{60}^+$ in TCE.

The ionization energy of $C_{60}$ is high because of *s* character in the $\pi$ system, induced by curvature (*20*). Chemically, electrophilic oxidants such as $Br_2$ and $Cl_2$ react with $C_{60}$ (*21*), but the products involve addition rather than oxidation because of the nucleophilicity of the halide ions that accompany the oxidizing equivalents. Thus, the characterization of $C_{60}^{\cdot+}$ to date has been restricted to the gas phase or to spectroscopy on transients (*22*). Attempts to prepare and characterize $C_{60}^{\cdot+}$ in oxidizing superacid media have met with limited indications of success (*8, 9, 23*).

The problem of oxidizing $C_{60}$ to $C_{60}^{\cdot+}$ is to find an oxidant that is strong enough (>1.26 V versus $Fc/Fc^+$) but that does not bring along a reacting nucleophile. We recently solved this problem for $C_{76}$, which is ~0.5 V easier to oxidize (*24*), but the repertoire of practical oxidizing reagents for organic media has been limited to oxidants of ~0.7 V for quite some time (*25*). A new oxidant based on a triarylaminium radical cation can be prepared from the hexabrominated phenylcarbazole, **1** (Scheme 2). The bromine substitution pattern in **1** was established by x-ray crystallography, mass spectrometry, and $^1H$ and $^{13}C$ NMR spectroscopy. Cyclic voltammetry in $CH_2Cl_2/Bu_4N^+PF_6^-$ shows a reversible anodic wave at 1.34 V versus $Fc/Fc^+$. Partnering the stable radical cation of **1** with the hexachlorocarborane anion $CB_{11}H_6Cl_6^-$ via $Cl_2$ oxidation in the presence of a silver carborane salt gives the purple-brown reagent $[\mathbf{1}^+][CB_{11}H_6Cl_6^-]$ [$\lambda_{max}$ = 1163 in ODCB; electron paramagnetic resonance (EPR): $g$ = 2.0107, $\Delta H_{pp}$ = 40 G in ODCB at 5 K].

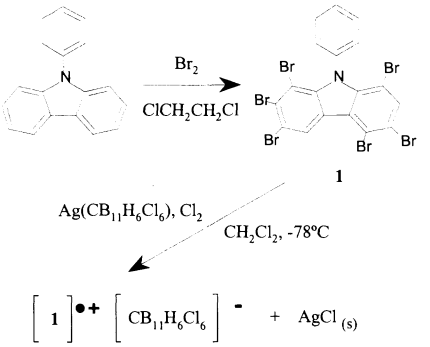


**Scheme 2.**

Treatment of $C_{60}$ with a slight molar excess of $[\mathbf{1}^+][CB_{11}H_6Cl_6^-]$ in carefully dried TCE or ODCB produces a dark red solution that is stable for several hours. The electronic absorption spectrum (Fig. 3D) shows minor changes in the visible region along with a diagnostic band at 980 nm in the near-IR region. This band has been identified with $C_{60}^{\cdot+}$ in low-temperature matrix isolation studies (*22, 26*). A weaker band appears at 847 nm with a shoulder at ~750 nm. The $^{13}C$ NMR spectrum in TCE is consistent with a radical cation. A broad singlet is observed at 144.2 ppm (linewidth ~340 Hz at half height; Fig. 4C). The downfield shift and broadening relative to $C_{60}$ (142.83 ppm, linewidth ~21 Hz) are the expected result of paramagnetism in a radical cation. Mixtures of $C_{60}$ and $C_{60}^{\cdot+}$ show peaks of averaged chemical shift and linewidth indicating that intermolecular electron transfer between them is fast on the NMR time scale. The EPR spectrum in frozen ODCB solution ($g$ = 2.002, $\Delta H_{pp}$ = 8 G at 5 K) is typical of a delocalized organic radical cation, showing none of the complexity observed with the radical anion, $C_{60}^{\cdot-}$ (*22*). Attempts to isolate pure crystalline salts have led to solids that contain both $[C_{60}^{\cdot+}][CB_{11}H_6X_6^-]$ ($g$ = 2.0022, $\Delta H_{pp}$ = 3 G at 105 K) and $C_{60}$. We hypothesize that concentration of the solution accelerates a bimolecular disproportionation reaction giving $C_{60}$ and the superelectrophile $C_{60}^{2+}$, which is immediately attacked by the solvent, counterion, or errant nucleophiles. This mechanism is well established for the decomposition of radical cations of aromatic hydrocarbons (*27*). Otherwise, the redox reaction is entirely reversible. Treatment of solutions of $[C_{60}^{\cdot+}][CB_{11}H_6X_6^-]$ with ($p$-$BrC_6H_4)_3N$ (E = 0.72 V) gives ($p$-$BrC_6H_4)_3N^+$ and $C_{60}$. The preparation of stable solutions of $C_{70}^{\cdot+}$ ($\lambda_{max}$ = 770 nm; $g$ = 2.0012, $\Delta H_{pp}$ = 4 G in ODCB at 10 K) can be carried out in a similar manner to $C_{60}^{\cdot+}$.

There are wider possibilities for the new oxidant and superacid reagents. The superacid $H(CB_{11}H_6X_6)$ is the rare example of a weighable reagent for the stoichiometric delivery of exceptionally clean protons to organic solvents at superacidity levels. Previously unobservable primary protonation reactions may now be amenable to study, and reactive cations observed only in solution at subambient temperatures may now be accessible as room temperature–stable salts, suitable for x-ray crystal structure determination (*12*). Stepwise protonation and purposeful addition of a selected nucleophile should allow easier exploration of acid-catalyzed processes. These reagents should also find applications in mechanistic studies, where dissection of the sequence of protonation, oxidation, and nucleophilic attack is desired. Another mechanistically useful property may be the strict separation of Brønsted and Lewis acidity achieved in $H(CB_{11}H_6X_6)$. In contrast to many superacids such as $HF/SbF_5$, $H(CB_{11}H_6X_6)$ is not a mixture of Brønsted and Lewis acids.

Finally, we note that this chemistry is possible because of the exceptional stability of the icosahedral boron cluster, possibly the most stable cluster in chemistry (*11*). The three-dimensional $\sigma$ aromaticity of the $CB_{11}$ framework resists disruption to the point that in the absence of good nucleophiles, the exohedral C–H, B–H, and B–X bonds are resistant to acid or oxidative cleavage. This inertness reduces the basicity and nucleophilicity of the anion to less than that of common halocarbon solvents such as ODCB. Superacidity, commonly associated with corrosive viscous liquids (e.g., "magic acid," $HSO_3F/SbF_5$), is thereby brought into the realm of standard solution chemistry with understandable properties.

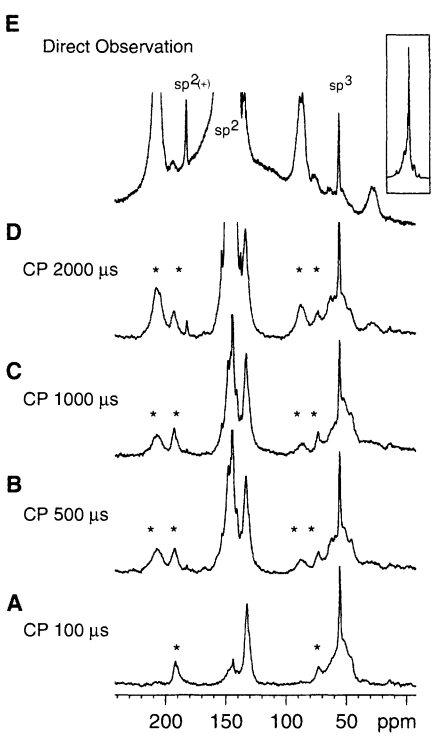


**Fig. 5.** Solid-state $^{13}C$ MAS NMR spectra of $[HC_{60}^+][CB_{11}H_6Cl_6^-]$. (**E**) Proton-decoupled (with insert showing the off-scale region at 133 to 154 ppm) and (**A** through **D**) $^1H$-$^{13}C$ cross-polarization (CP) experiments with increasing contact times. Peaks marked with asterisks are spinning sidebands.

### References and Notes


1. G. A. Olah, G. K. S. Prakash, J. Sommer, *Superacids* (Wiley-Interscience, New York, 1985).
2. P. J. F. de Rege, J. A. Gladysz, I. T. Horvath, *Science* **276**, 776 (1997).
3. R. J. Gillespie and J. Passmore, *Adv. Inorg. Chem. Radiochem.* **17**, 49 (1975) .
4. T. A. O'Donnell, *Superacids and Acidic Melts as Inorganic Chemical Reaction Media* (VCH, Weinheim, Germany, 1993).
5. H. Willner and F. Aubke, *Angew. Chem. Int. Ed. Engl.* **36**, 2402 (1997).
6. T. Drews and K. Seppelt, *Angew. Chem. Int. Ed. Engl.* **36**, 273 (1997).
7. C. A. Reed, *Acc. Chem. Res.* **31**, 325 (1998).
8. J. W. Bausch *et al.*, *J. Am. Chem. Soc.* **113**, 3205 (1991).
9. F. Cataldo, *Spectrochim. Acta A* **51**, 405 (1995).
10. F. Wudl, *Acc. Chem. Res.* **25**, 157 (1992).
11. C. A. Reed, *Acc. Chem. Res.* **31**, 133 (1998).
12. C. A. Reed *et al.*, *J. Am. Chem. Soc.* **121**, 6314 (1999).
13. J. F. Haw, J. B. Nicholas, T. Xu, L. W. Beck, D. B. Ferguson, *Acc. Chem. Res.* **29**, 259 (1996).

14. T. Kitagawa, H. Sakamoto, K. Takeuchi, *J. Am. Chem. Soc.* **121**, 4298 (1999).
15. We find that $C_{60}(CHCl_2)^+$ is produced when $H(CB_{11}H_6Br_6)$ reacts with $C_{60}$ in dichloromethane (Fig. 3C), presumably via protonation of dichloromethane, loss of $H_2$ to form $CHCl_2^+$, and addition of this carbocation to $C_{60}$.
16. C. C. Henderson and P. A. Cahill, *Science* **259**, 1885 (1993).
17. G. A. Olah *et al.*, *J. Am. Chem. Soc.* **100**, 6299 (1978).
18. G.-W. Wang, K. Komatsu, Y. Murata, M. Shiro, *Nature* **387**, 583 (1997).
19. Q. Xie, F. Arias, L. Echegoyen, *J. Am. Chem. Soc.* **115**, 9818 (1993).
20. R. C. Haddon, *Acc. Chem. Res.* **25**, 127 (1992).
21. R. Taylor, *Lecture Notes in Fullerene Chemistry* (Imperial College Press, London, 1999).
22. C. A. Reed and R. D. Bolskar, *Chem. Rev.* **100**, 1075 (2000).
23. G. P. Miller, C. S. Hsu, H. Thomann, L. Y. Chiang, M. Bernardo, *Mater. Res. Soc. Symp. Proc.* **247**, 293 (1992).
24. R. D. Bolskar, R. S. Mathur, C. A. Reed, *J. Am. Chem. Soc.* **118**, 13093 (1996).
25. N. G. Connelly and W. E. Geiger, *Chem. Rev.* **96**, 877 (1996).
26. T. Kato *et al.*, *Chem. Phys. Lett.* **180**, 446 (1991).
27. A. J. Bard, A. Ledwith, H. J. Shine, *Adv. Phys. Org. Chem.* **13**, 155 (1976).
28. This paper is dedicated to G. A. Olah who stimulated our interest in carbocations. We thank D. Stasko and N. Fackler for their contributions to this project. Supported by NSF grants CHE-9996002 to C.A.R. and CHE-9982362 to L.J.M. and NIH grant GM23851 to C.A.R.

10 April 2000; accepted 17 May 2000

# Subducted Seamount Imaged in the Rupture Zone of the 1946 Nankaido Earthquake

**Shuichi Kodaira, Narumi Takahashi, Ayako Nakanishi, Seiichi Miura, Yoshiyuki Kaneda**

**The Nankai Trough is a vigorous subduction zone where large earthquakes have been recorded since the seventh century, with a recurrence time of 100 to 200 years. The 1946 Nankaido earthquake was unusual, with a rupture zone estimated from long-period geodetic data that was more than twice as large as that derived from shorter period seismic data. In the center of this earthquake rupture zone, we used densely deployed ocean bottom seismographs to detect a subducted seamount 13 kilometers thick by 50 kilometers wide at a depth of 10 kilometers. We propose that this seamount might work as a barrier inhibiting brittle seismogenic rupture.**

Large subduction zone earthquakes have repeatedly occurred along the Nankai Trough, in southwest Japan, where the Philippine Sea Plate is subducting beneath Japan. Recurrence intervals and areas affected by these earthquakes have been documented since the seventh century (*1*). According to the historical literature, almost the entire length of the Nankai Trough (500 km) has been ruptured every 100 to 200 years by one or two successive large earthquakes. The most recent events, the 1944 Tonankai and 1946 Nankaido earthquakes, are the best studied of the large Nankai Trough earthquakes (*2–5*). The seismic data and geodetic data yield two conflicting results concerning the rupture process of the 1946 Nankaido earthquake. The geodetic data show a rupture area of $2.5 \times 10^4$ km$^2$ with a slip of 5 to 18 m (*3*), whereas the seismic data show a rupture area of $1 \times 10^4$ km$^2$ with a slip of 3 m (*4*). The area of the fault derived from the seismic data corresponds to the 1-day aftershock area (*5*), which is located in the eastern half of the fault area determined by the geodetic data.

We performed a high-resolution deep seismic study in the proposed rupture zone (Fig. 1) to investigate the rupture process of the Nankaido earthquake. We used refraction data generated by a large air gun along a profile (Fig. 1) running in the center of the rupture zone (*2*) at the western edge of the 1-day aftershock area (*5*). To resolve the seismic velocity structure with high resolution to depths of 10 to 30 km, we deployed 98 ocean bottom seismographs (OBSs) with a spacing of 1.6 km on the 185-km-long profile. This spacing of the OBSs is closer than in conventional seismic refraction surveys by a factor of more than 10. All OBSs were positioned at sea bottom by means of a super short baseline (SSBL) acoustic positioning system.

All observed record sections (Fig. 2) showed first arrivals (*P*-wave refraction arrivals) throughout the entire profile, except for OBSs deployed in shallow water

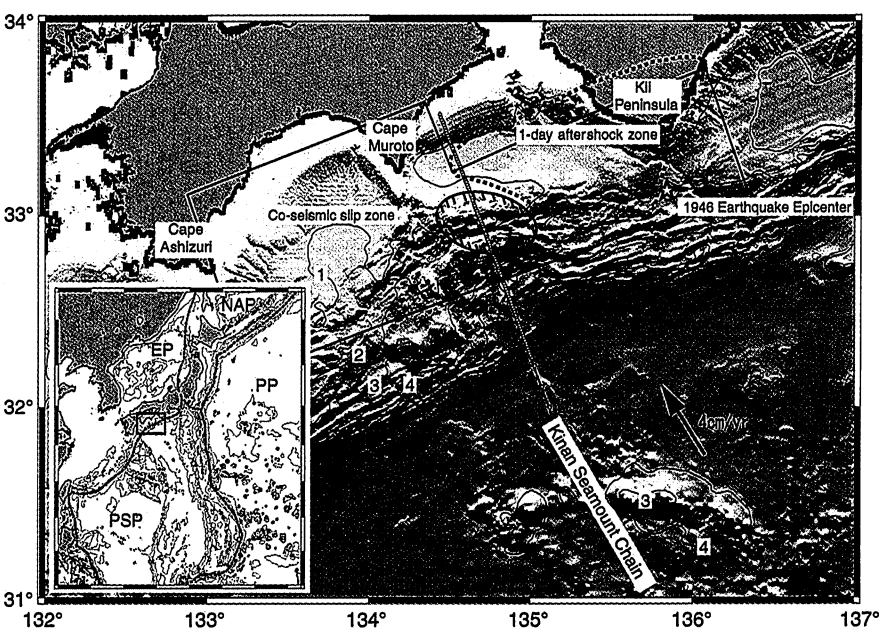


**Fig. 1.** Topography of the western part of the Nankai Trough and location of high-resolution deep seismic profile. Contour values denote water depth at 1-km intervals. The 1-day aftershock area (*5*) and rupture zone (*2*) derived from geodetic data are shown as dotted and solid lines, respectively. Except for the southern end of the profile, the 98 OBSs (yellow dots) were deployed with 1.6-km spacing. An ellipse on the profile shows the location of the subducted seamount detected by this study. The off-profile dimensions of the seamount are estimated by reference to the size of one of the Kinan seamounts located at the southeastern extension of the profile. The subducted seamount is located immediately outside of the 1-day aftershock zone of the 1946 Nankaido earthquake. The convergence rate of the Philippine Sea Plate under the Eurasian Plate is 4 cm/year (*18*). Topography data used were compiled by the Hydrographic Department, Japan Maritime Safety Agency (*19*). Inset abbreviations: EP, Eurasian Plate; NAP, North American Plate; PP, Pacific Plate; and PSP, Philippine Sea Plate.

Japan Marine Science and Technology Center, Natsushima 2-15, Yokosuka, Kanagawa 237-0061, Japan.